

# 2 V-Operated InGaP–AlGaAs–InGaAs Enhancement-Mode Pseudomorphic HEMT

L. H. Chu, E. Y. Chang, *Senior Member, IEEE*, S. H. Chen, Y. C. Lien, and C. Y. Chang, *Fellow, IEEE*

**Abstract**—A low-voltage single power supply enhancement-mode InGaP–AlGaAs–InGaAs pseudomorphic high-electron mobility transistor (PHEMT) is reported for the first time. The fabricated  $0.5 \times 160 \mu\text{m}^2$  device shows low knee voltage of 0.3 V, drain–source current ( $I_{\text{DS}}$ ) of 375 mA/mm and maximum transconductance of 550 mS/mm when drain–source voltage ( $V_{\text{DS}}$ ) was 2.5 V. High-frequency performance was also achieved; the cut-off frequency ( $F_t$ ) is 60 GHz and maximum oscillation frequency ( $F_{\text{max}}$ ) is 128 GHz. The noise figure of the 160- $\mu\text{m}$  gate width device at 17 GHz was measured to be 1.02 dB with 10.12 dB associated gain. The E-mode InGaP–AlGaAs–InGaAs PHEMT exhibits a high output power density of 453 mW/mm with a high linear gain of 30.5 dB at 2.4 GHz. The E-mode PHEMT can also achieve a high maximum power added efficiency (PAE) of 70%, when tuned for maximum PAE.

**Index Terms**—Enhancement mode, InGaP, InGaP–InGaAs, PHEMT, single-voltage supply.

## I. INTRODUCTION

FOR cellular phone applications, microwave devices require high power-added efficiency (PAE) and high output power operated at low dc power supply [1]. Enhancement-mode pseudomorphic high electron mobility transistors (E-mode PHEMTs) are suitable for cellular phone applications due to their single voltage supply operation and their low knee voltage characteristic. These advantages can reduce the dc power consumption, improve the efficiency, and increase the operation time. In the past few years, many reports on the enhancement-mode AlGaAs–InGaAs PHEMTs have quoted high-power density and high PAE at low-voltage operation [2]–[4].

Recently, the use of InGaP instead of AlGaAs in the device structure has become very popular [5]–[7]. The InGaP–InGaAs PHEMTs have many advantages over the AlGaAs–InGaAs PHEMTs. These include excellent etching selectivity between InGaP and GaAs, which increases the device manufacturability, and high energy bandgap of InGaP, which results in low microwave noise and reduces the Gunn oscillation effects [5]. In addition, InGaP does not form DX-center, and causes less

deep level defects, which has great potential to improve the reliability of the PHEMTs [6], [8].

In this letter, InGaP–AlGaAs–InGaAs PHEMTs were developed to further enhance the device performance. The attempt to use InGaP–AlGaAs–InGaAs heterojunction instead of InGaP–InGaAs is due to: First, the conduction band discontinuity of the AlGaAs–InGaAs interface is greater than the InGaP–InGaAs interface [9], the carrier confinement is better, which will improve the output power performance of the InGaP PHEMTs. Second, an  $\text{In}_{0.49}\text{Ga}_{0.51}\text{P}_x\text{As}_{1-x}$  layer exists in the InGaP–InGaAs interface due to the intermixing behavior of As and P atoms during the growth [10]. The formation of a parasitic well in the interface reduced the electron mobility due to the trapping effect of the transferred electrons in the parasitic well [11]. As a result, the Hall mobility of the InGaP–AlGaAs–InGaAs PHEMTs is higher than the InGaP–InGaAs PHEMTs [12]. In this letter, the electron mobility of the InGaP–AlGaAs–InGaAs structure is  $6410 \text{ cm}^2/\text{Vs}$  at room temperature.

## II. DEVICE STRUCTURE AND FABRICATION

The E-mode InGaP–AlGaAs–InGaAs PHEMT structure was grown by the metal–organic chemical vapor deposition method on a 4-in GaAs substrate. The device structure was composed of, from bottom to top, 2500-Å GaAs buffer layer, 2200-Å GaAs–AlGaAs super-lattice, 200-Å  $\text{Al}_{0.24}\text{Ga}_{0.76}\text{As}$  layer, followed by undoped 30-Å  $\text{Al}_{0.24}\text{Ga}_{0.76}\text{As}$  spacer, lower Si  $\delta$ -doped layer, 100-Å  $\text{In}_{0.2}\text{Ga}_{0.8}\text{As}$  channel, 30-Å  $\text{Al}_{0.24}\text{Ga}_{0.76}\text{As}$  spacer, upper Si  $\delta$ -doped layer, 120-Å undoped  $\text{In}_{0.49}\text{Ga}_{0.51}\text{P}$  layer and 700-Å heavily doped  $\text{n}^+$  GaAs cap layer. The epi-structure of the device is as shown in Fig. 1. The  $\text{In}_{0.49}\text{Ga}_{0.51}\text{P}$  layer was used as the Schottky layer, and the InGaP layer also achieved a high etching selectivity with the GaAs layer during the cap layer etching process. The mesa isolation was done by wet chemical etching. Ohmic contacts were formed by evaporating Au–Ge–Ni–Au on  $\text{n}^+$  GaAs layer and then alloyed at 350 °C using rapid thermal annealing. The contact resistance measured by the transmission line model method was  $1 \times 10^{-6} \Omega\text{-cm}^2$ . For T-gate definition, the bi-layer resist structure consisting of polymethylmethacrylate and polymethyl methacrylate-methacrylic were exposed by E-beam lithography (Leica EBML300) with a footprint of 0.5  $\mu\text{m}$ . Citric acid– $\text{H}_2\text{O}$ – $\text{H}_2\text{O}_2$  solution were used for gate recess process, and the recess was stopped at the InGaP layer. Then, gate metals Ti–Pt–Au (100/100/300 nm) were deposited sequentially as the Schottky metal of the T-shaped gate. After T-gate formation, 100-nm-thick silicon nitride film was deposited by plasma enhanced chemical vapor deposition as the

Manuscript received August 23, 2004; revised November 8, 2004. This work was supported by the National Science Council, Taiwan, R.O.C., under Contract NSC 93-2752-E-09-003-PAE and Contract 93-EC-17-A-05-S1-020. The review of this letter was arranged by Editor D. Ritter.

L. H. Chu, E. Y. Chang, S. H. Chen, and Y. C. Lien are with the Department of Materials Science and Engineering, National Chiao-Tung University, Hsinchu 300, Taiwan, R.O.C. (e-mail: edc@mail.nctu.edu.tw).

C. Y. Chang is with the Department of Electronics Engineering, National Chiao-Tung University, Hsinchu 300, Taiwan, R.O.C.

Digital Object Identifier 10.1109/LED.2004.841184

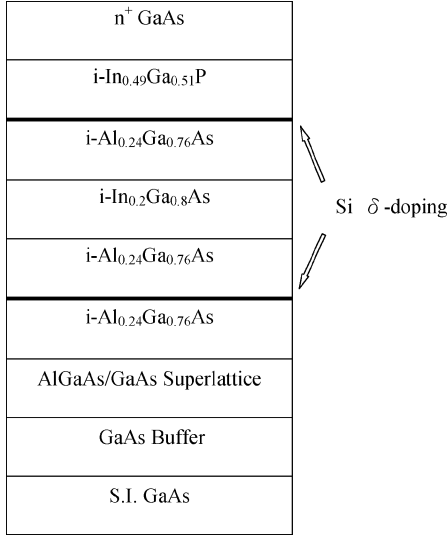


Fig. 1. Device structure of the enhancement-mode InGaP–AlGaAs–InGaAs PHEMT.

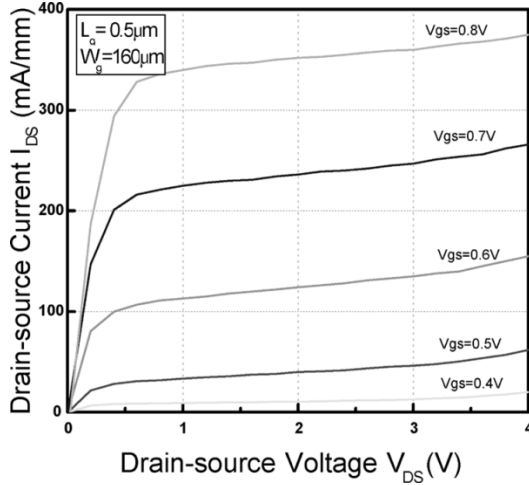


Fig. 2.  $I$ - $V$  characteristics of the  $0.5 \mu\text{m} \times 160 \mu\text{m}$  E-mode InGaP–AlGaAs–InGaAs PHEMT.

passivation layer. Finally,  $2\text{-}\mu\text{m}$ -thick Au plated air-bridges were formed for multifinger device interconnections.

### III. DEVICE PERFORMANCE

The current–voltage ( $I$ - $V$ ) characteristics of the fabricated  $0.5 \times 160 \mu\text{m}^2$  E-mode InGaP–AlGaAs–InGaAs PHEMTs as shown in Fig. 2. The drain–to–source current ( $I_{\text{DS}}$ ) was  $375 \text{ mA/mm}$  at  $V_{\text{GS}} = 0.8 \text{ V}$  and a low knee voltage of  $0.3 \text{ V}$ . The device has a threshold voltage ( $V_{\text{th}}$ ) of  $0.14 \text{ V}$  with small standard deviation of  $30 \text{ mV}$  across the  $4\text{-in}$  wafer. The threshold voltage is defined as  $V_{\text{GS}}$  when the  $I_{\text{DS}}$  is  $1 \text{ mA/mm}$ . The high threshold voltage uniformity of the E-mode PHEMT was due to the high etching selectivity between InGaP and GaAs layer. The maximum transconductance measured at  $V_{\text{DS}} = 2.5 \text{ V}$  was  $550 \text{ mS/mm}$ , as shown in Fig. 3. The drain–to–gate breakdown voltage ( $V_{\text{BK}}$ ) was  $10 \text{ V}$ , which was defined at a gate current of  $1 \text{ mA/mm}$ .

For RF performance, the  $S$  parameters of the E-mode PHEMTs were measured by on-wafer testing from  $1$  to  $35$

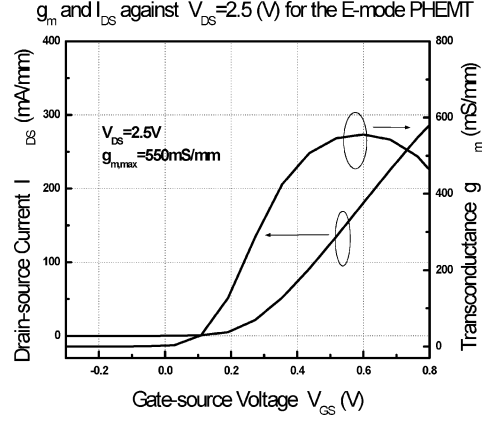


Fig. 3. Transconductance and drain–source current versus  $V_{\text{GS}}$  of the  $0.5 \times 160 \mu\text{m}$  E-mode PHEMT.

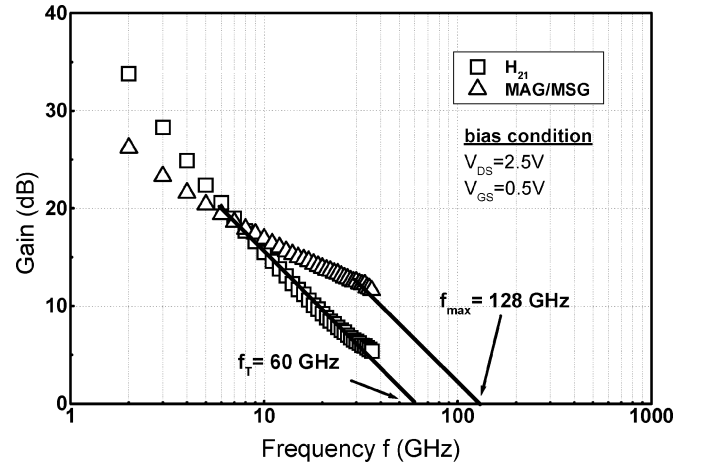


Fig. 4. Typical  $H_{21}$ , and MAG/MSG, as a function of the frequency for the  $0.5 \times 160 \mu\text{m}$  E-mode PHEMT biased at  $V_{\text{DS}} = 2.5 \text{ V}$  and  $V_{\text{GS}} = 0.5 \text{ V}$ .

GHz. The current gain ( $H_{21}$ ) and the maximum available gain/maximum stable gain (MAG/MSG) as a function of frequency are shown in Fig. 4. The calculated  $f_T$  and  $f_{\text{max}}$  of the E-mode PHEMT measured at the  $V_{\text{DS}} = 2.5 \text{ V}$  and  $V_{\text{GS}} = 0.5 \text{ V}$  were  $60 \text{ GHz}$  and  $128 \text{ GHz}$ , respectively, by a  $-20 \text{ dB/decade}$  slope extrapolation. The outstanding RF performance of the Enhancement-mode device is due to the use of InGaP–AlGaAs–InGaAs heterojunction which produce high electron mobility in the channel region. The measured minimum noise figure ( $F_{\text{min}}$ ) was  $1.02 \text{ dB}$  with  $10.12 \text{ dB}$  associated gain at  $17 \text{ GHz}$  under  $V_{\text{DS}} = 2 \text{ V}$  and  $V_{\text{GS}} = 0.3 \text{ V}$ .

The power performance measurement was also performed by an ATN load-pull system. The power performances of the  $0.5 \times 160 \mu\text{m}^2$  devices measured at  $2.4 \text{ GHz}$  are shown in Fig. 5(a). When tuned for maximum PAE match, the output power ( $P_{\text{out}}$ ) was  $10.88 \text{ dBm}$  and the maximum PAE was  $70\%$ , when the dc bias condition was  $V_{\text{DS}} = 2 \text{ V}$ ,  $V_{\text{GS}} = 0.2 \text{ V}$ . If the device was biased at  $V_{\text{DS}} = 2 \text{ V}$ ,  $V_{\text{GS}} = 0.4 \text{ V}$  and tuned for maximum output power match, the output power ( $P_{\text{out}}$ ) of  $18.61 \text{ dBm}$  ( $453 \text{ mW/mm}$ ) with  $32.5\%$  PAE was obtained and the device had a linear gain of  $30.5 \text{ dB}$ , as shown in Fig. 5(b). Overall, the state-of-the-art, InGaP–AlGaAs–InGaAs E-mode PHEMT is demonstrated with a much lower operating voltage than the reported AlGaAs–InGaAs [1]–[4] and InGaP–InGaAs

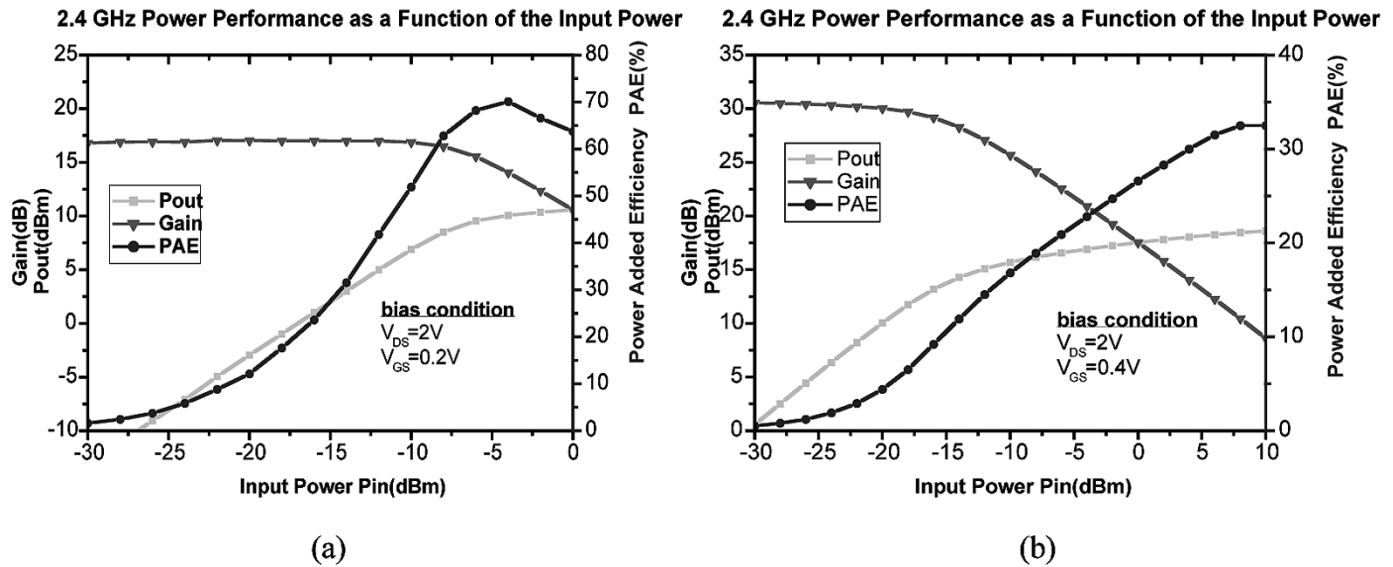


Fig. 5. The 2.4 GHz power performance as a function of the input power for the  $0.5 \times 160 \mu\text{m}$  E-mode PHEMT. (a)  $V_{DS} = 2\text{ V}$ ,  $V_{GS} = 0.2\text{ V}$ . The device was tuned for maximum PAE. (b)  $V_{DS} = 2\text{ V}$ ,  $V_{GS} = 0.4\text{ V}$ . The device was tuned for maximum output power.

E-mode PHEMTs [5], [10]. The developed E-mode InGaP PHEMT shows excellent dc and RF performance. We believed the improved device performance is the results of the introduction of the InGaP–AlGaAs–InGaAs heterojunction.

#### IV. CONCLUSION

A single-voltage supply, high frequency and high-power density Enhancement-mode InGaP–AlGaAs–InGaAs PHEMT was developed for low-voltage wireless application. The calculated  $f_T$  and  $f_{max}$  of the E-mode PHEMT were 60 and 128 GHz. The  $F_{min}$  at 17 GHz was measured to be 1.02 dB with 10.12 dB associated gain. High power performance was achieved, the E-mode PHEMT exhibited maximum PAE of 70%, and maximum power density of 453 mW/mm at 2.4 GHz. The excellent threshold voltage uniformity and performance of the E-mode PHEMT were due to the use of InGaP–AlGaAs–InGaAs layer structure which took advantages of high etching selectivity between InGaP–GaAs and high electron mobility due to the use of AlGaAs spacer layer.

#### ACKNOWLEDGMENT

The authors would like to thank the National Nano Device Laboratories RF group for  $S$ -parameter measurements.

#### REFERENCES

[1] S. Yoshida, Y. Wakabayashi, M. Kohno, and K. Uemura, "Greater than 70% PAE enhancement-mode GaAs HJFET power amplifier MMIC with extremely low leakage current," in *IEEE MTT-S Dig.*, vol. 3, 1999, pp. 1183–1186.

[2] D.-W. Wu, R. Parkhurst, S.-L. Fu, J. Wei, C.-Y. Su, S.-S. Chang, D. Moy, W. Fields, P. Chye, and R. Levitsky, "A 2 W, 65% PAE single-supply enhancement-mode power PHEMT for 3 V PCS applications," in *IEEE MTT-S Dig.*, 1997, pp. 1319–1322.

[3] Y. Bito, T. Kato, and N. Iwata, "Enhancement-mode power heterojunction FET utilizing  $\text{Al}_{0.5}\text{Ga}_{0.5}\text{As}$  barrier layer with negligible operation gate current for digital cellular phones," *IEEE Trans. Electron Devices*, vol. 48, no. 8, pp. 1503–1509, Aug. 2001.

[4] S. Zhang, J. Cao, and R. Mcmorrow, "E-PHEMT, single supply, high efficient power amplifiers for GSM and DCS applications," in *MTT-S Dig.*, 2001, pp. 927–930.

[5] H. K. Huang, Y. H. Wang, C. L. Wu, J. C. Wang, and C. S. Chang, "Super low noise InGaP gated PHEMT," *IEEE Electron Device Lett.*, vol. 23, no. 2, pp. 70–72, Feb. 2002.

[6] T. Takahashi, S. Sasa, A. Kawano, T. Iwai, and T. Fuji, "High-reliability InGaP–GaAs HBTs fabricated by self-aligned process," in *IEDM Tech. Dig.*, 1994, pp. 191–194.

[7] E. Lan, B. Pitts, M. Mikhov, and O. Hartin, "InGaP PHEMTs for wireless power application," in *Proc. IEEE MTT-S*, 2001, pp. 22155–2157.

[8] M.-Y. Kao, E. A. Beam III, P. Saunier, and W. R. Frensley, "X-band InGaP PHEMTs with 70% power-added efficiency," in *Proc. IEEE MTT-S*, vol. 3, 1998, pp. 1671–1674.

[9] M. Missous, A. A. Aziz, and A. Sandhu, "InGaP–InGaAs–GaAs high electron mobility transistor structure grown by solid source molecular beam epitaxy using GaP as phosphorous source," *Jpn. J. Appl. Phys.*, vol. 36, pp. L647–L649, 1997.

[10] F. E. G. Guimaraes, B. Elsner, R. Westphalen, B. Spangenberg, H. J. Geelen, P. Balk, and K. Heime, "LP-MOVPE growth and optical characteristic of InGaP–GaAs heterostructure: Interface, quantum wells and quantum wires," *J. Cryst. Growth*, vol. 124, p. 199, 1992.

[11] O. Schuler, O. Dehaese, X. Wallart, and F. Mollot, *J. Appl. Phys.*, vol. 84, p. 765, 1998.

[12] H. Q. Zheng, S. F. Yoon, B. P. Gay, K. W. Mah, K. Radhakrishnan, and G. I. Ng, "Growth optimization of InGaP layers by solid source molecular beam epitaxy for the application of InGaP– $\text{In}_{0.2}\text{Ga}_{0.8}\text{As}$ -GaAs high electron mobility transistor structures," *J. Cryst. Growth*, vol. 216, pp. 51–56, 2000.